DEVELOPMENTAL BIOLOGY

# Dlp-mediated Hh and Wnt signaling interdependence is critical in the niche for germline stem cell progeny differentiation

**Renjun Tu[1], Bo Duan[1], Xiaoqing Song[1], Ting Xie[1,2]***



**Although multiple signaling pathways work synergistically in various niches to control stem cell self-renewal and differentiation, it remains poorly understood how they cooperate with one another molecularly. In the *Drosophila* ovary, Hh and Wnt pathways function in the niche to promote germline stem cell (GSC) progeny differentiation. Here, we show that glypican Dlp-mediated Hh and Wnt signaling interdependence operates in the niche to promote GSC progeny differentiation by preventing BMP signaling. Hh/Wnt-mediated *dlp* repression is essential for their signaling interdependence in niche cells and for GSC progeny differentiation by preventing BMP signaling. Mechanistically, Hh and Wnt downstream transcription factors directly bind to the same *dlp* regulatory region and recruit corepressors composed of transcription factor Croc and Egg/H3K9 trimethylase to repress Dlp expression. Therefore, our study reveals a novel mechanism for Hh/Wnt signaling–mediated direct *dlp* repression and a novel regulatory mechanism for Dlp-mediated Hh/Wnt signaling interdependence in the GSC differentiation niche.**

## INTRODUCTION

Stem cells in adult tissue undergo lifelong continuous self-renewal and generate differentiated cells for maintaining tissue homeostasis by replenishing the lost cells caused by natural turnover, aging, injury, or disease. Adult stem cell self-renewal and proliferation are demonstrated to be controlled by the niche in various tissues and organisms (*1*, *2*). Studies on stem cells from different organisms ranging from *Drosophila* to mammals have demonstrated that one or multiple signals originated from the niche directly act on stem cells in concert with varieties of different intrinsic factors to control stem cell self-renewal by repressing differentiation pathways (*1*, *2*). Our recent study on germline stem cells (GSCs) in the *Drosophila* ovary has also demonstrated that stem cell progeny differentiation is also controlled extrinsically by the niche formed by adjacent stromal cells, which is named as the differentiation niche (*3*). Resident macrophage cells on the surface seminiferous tubule in the adult mouse testis also contribute to the niche for regulating germ cell differentiation, suggesting that the niche dedicated to differentiation might also exist in mammalian tissues (*4*). Multiple signaling pathways are usually used by niches in various stem cell systems to control either self-renewal or differentiation, but how they cooperate with one another in niches to control stem cell behavior remains poorly understood. In this study, we show that Hh and Wnt signaling pathways use novel cooperative mechanisms to provide the favorable environment for GSC progeny differentiation in the *Drosophila* ovary by maintaining each other's signaling activities.

The *Drosophila* ovary provides an effective system for studying stem cell self-renewal and differentiation due to well-defined GSCs and niches. Two or three GSCs physically interact with the niche consisting of primarily cap cells, whereas early GSC progeny physically interact with their own niche composed of inner germarial sheath (IGS) cells (also known as escort cells) (fig. S1A) (*5*, *6*). The GSCs located at the tip of the germarium continuously generate cystoblasts (CBs), which can further divide four times synchronously with incomplete cytokinesis to form mitotic cysts (2-cell, 4-cell, and 8-cell) and 16-cell cysts. Cap cells and anterior row of IGS cells directly contact GSCs and form the niche for promoting self-renewal (*7*–*10*). The niche uses bone morphogenetic protein (BMP) signaling and E-cadherin–mediated cell adhesion to control GSC self-renewal and proliferation (*5*). In 2011, IGS cells were first proposed to form a niche for promoting GSC progeny differentiation (*3*). Thus, two distinct niche compartments control stem cell self-renewal and differentiation separately.

IGS cells function as the differentiation niche for GSC progeny through physical interactions and signaling. IGS cells extend long cellular processes to encase early differentiating GSC progeny, including CBs, mitotic cysts, and 16-cell cysts (*3*, *11*). Further genetic studies have demonstrated that IGS cellular process–mediated physical interactions are essential for promoting GSC progeny differentiation (*3*, *9*, *12*, *13*). In addition, different signaling pathways and gene networks have been identified for their requirement in IGS cells for promoting GSC progeny differentiation by preventing BMP signaling through distinct mechanisms (*5*). Notably, epidermal growth factor receptor (EGFR), Wnt, Hh, and Jak-Stat signaling pathways are required in IGS cells to promote GSC progeny differentiation by preventing BMP signaling via regulation of *dally*, *dpp*, or both (*12*, *14*–*21*). *dally* encodes a proteoglycan protein promoting the diffusion of Dpp/BMP protein in *Drosophila* (*22*). In addition to repressing BMP signaling, IGS cells might also send direct signals to GSC progeny to promote their differentiation, but these signals remain to be defined. In contrast, EGFR signaling has so far been reported to be required in adult somatic cysts to promote GSC progeny differentiation in the *Drosophila* testis (*23*).

Since both Hh and Wnt signaling pathways are required in IGS cells for promoting GSC progeny differentiation by repressing BMP signaling, their functional relationship in the niche remains unclear. This study has revealed that they are dependent on each other for their activities in IGS cells through repressing *dally-like protein* (*dlp*). *dlp* encodes a Dally-related glypican (GPC) protein, which is known to promote BMP, Hh, and Wnt signaling in *Drosophila* (*24*). However, Dlp-related GPCs can both promote and inhibit Shh and

[1]Stowers Institute for Medical Research, 1000 East 50th Street, Kansas City, MO 64110, USA. [2]Department of Anatomy and Cell Biology, University of Kansas Medical Center, Kansas City, KS 66160, USA.
*Corresponding author. Email: tgx@stowers.org

Wnt signaling in mammals (*25*–*27*). Here, we show that Dlp up-regulation can sufficiently inhibit both Hh and Wnt signaling and elevate BMP signaling. *dlp* knockdown in IGS cells can significantly rescue the GSC progeny differentiation defects caused by defective Hh or Wnt signaling and can also uncouple the interdependence of Hh and Wnt signaling. Hh and Wnt signaling directly repress *dlp* expression through recruiting Croc and H3K9 trimethylase Eggless into the regulatory region. Therefore, this study has revealed a novel cooperative mechanism of Hh and Wnt signaling and a novel Hh/Wnt-mediated mechanism for *dlp* repression in the niche for preventing BMP signaling and promoting GSC progeny differentiation.

## RESULTS

### Hh and Wnt signaling activities are mutually dependent in the niche

Hh and Wnt signaling are both required in IGS cells for proper GSC progeny differentiation. To investigate the relationship between Hh and Wnt signaling in IGS cells, we examined the expression of *ptc*–green fluorescent protein (GFP) and *fz3*–red fluorescent protein (RFP), which are Hh and Wnt signaling activity reporters, respectively (*28*–*30*), in adult *smo* and *dsh* knockdown (*smoKD* and *dshKD*) IGS cells. IGS-expressed *gal4* line, *c587*, is combined with a temperature-sensitive mutant *gal80* (*gal80*$^{ts}$) to achieve RNA interference (RNAi)–mediated gene knockdown in adult IGS cells after shifting adult flies from room temperature to 29°C (fig. S1B) (*12*, *15*). Two independent RNAi lines for *smo* and *dsh*, which had been characterized previously (*12*, *15*), were used to inactivate Hh or Wnt signaling in this study, respectively. The enhancer trap line PZ1444 expressing nuclear LacZ is used to label IGS cells and cap cells, which can further be distinguished on the basis of their distinct nucleus size and location (*15*). Consistent with our previous finding that Hh and Wnt signaling are required for IGS maintenance, most of IGS cells are lost 5 and 7 days after *dsh* or *smo* knockdown (fig. S1, C and D). However, IGS numbers remain close to normal 2 days after their knockdown, which is the time when we examined *fz3*-RFP and *ptc*-GFP expression throughout this study (fig. S1, C and D, and Fig. 1, A and B).

On the basis of *fz3*-RFP and *ptc*-GFP expression, knocking down *smo* or *dsh* for 2 days can effectively inactivate Hh and Wnt signaling in adult IGS cells, respectively (Fig. 1, A to D). Adult *dshKD* IGS cells significantly decrease *ptc*-GFP expression, while *smoKD* IGS cells significantly reduce *fz3*-RFP expression, indicating that Hh and Wnt signaling regulate each other (Fig. 1, A to D). Our previous RNA sequencing (RNA-seq) results on purified *dshKD* IGS cells did not show significant changes in *fz3* and *ptc* mRNAs compared with control IGS cells (table S1) (*15*). One of the concerns is that enzymatic dissociation of IGS cells destroys Hh and Wnt proteins in the extracellular space, which result in the loss of Hh and Wnt signaling in control IGS cells. As the whole IGS purification process lasts about 4 hours, which might be long enough for *fz3* and *ptc* mRNA decay, fluorescence-activated cell sorting (FACS)–purified control and *dshKD* IGS cells behave similarly on *fz3* and *ptc* mRNA levels. In the future, it should be extremely cautious to use FACS-purified cells for examining gene expression changes caused by secreted factors. Then, we performed fluorescent mRNA in situ hybridization (FISH) using quantitative hybridization chain reaction technology to further examine *fz3* and *ptc* mRNA expression changes in *dshKD* or *smoKD* IGS cells (*31*). *dshKD* or *smoKD* significantly decreases the expression of both *fz3* and *ptc* mRNAs in IGS cells (Fig. 1, E to H). To exclude the possibility that germ cell defects cause the loss of *fz3*-RFP and *ptc*-GFP expression in IGS cells, we examine *fz3*-RFP and *ptc*-GFP expression in IGS-specific *tkv* knockdown germaria, which exhibit the severe germ cell differentiation defect as reported previously (fig. S1, E and F) (*18*, *32*). *fz3*-RFP and *ptc*-GFP expression remain normal in *tkvKD* IGS cells despite the presence of the severe differentiation defect (fig. S1, E and F). Together, these results indicate that Wnt and Hh signaling are mutually dependent in IGS cells.

### Hh and Wnt signaling in the niche repress the expression of *dlp*, whose up-regulation sufficiently represses Hh and Wnt signaling

To investigate the mechanism underlying the Hh and Wnt signaling interdependence, we examined the previous RNA-seq results on purified control and *dshKD* IGS cells (*15*). dlp mRNA is up-regulated by about fourfold, but *dally* expression remains unchanged, in *dshKD* IGS cells compared with control ones (fig. S2A and table S1). *dally* and *dlp* encode highly related glypican proteins known to modulate Dpp/BMP, Hh, and Wnt signaling in *Drosophila* (*24*). Although its mRNA and protein levels are very low in control IGS cells, *dlp* mRNA and protein levels are drastically up-regulated in *dshKD* and *smoKD* IGS cells based on FISH and immunostaining results, respectively (fig. S2, B and C, and Fig. 2, A and B). These results reveal that Hh and Wnt signaling are required in IGS cells to repress Dlp expression.

Then, we determined whether *dlp* up-regulation in IGS cells can affect GSC progeny differentiation, Hh and Wnt signaling. In contrast with the control germaria containing about one CB, the 5- and 10-day Dlp-overexpressing (*dlpOE*) germaria accumulate approximately 10 and 20 spectrosome-containing single germ cells (SGCs), respectively, indicating that Dlp overexpression blocks CB differentiation (Fig. 2, C and D). *dlp* overexpression also diminishes the expression of *fz3*-RFP and *ptc*-GFP in IGS cells, indicating that Dlp up-regulation can sufficiently repress both Hh and Wnt signaling activities in the niche (Fig. 2, E to H). Dlp is known to be directly associated with Dpp, Hh, and Wg proteins to modulate their signaling activity (*22*, *26*, *33*, *34*), but it remains undermined whether Dlp can also directly bind to Wnt2 and Wnt4, two highly expressed Wnt proteins in IGS cells (*15*). We used coimmunoprecipitation (co-IP) experiments in S2 cells to show that Dlp can also be associated with Wnt2 and Wnt4 (fig. S2, D to G). Together, our findings indicate that up-regulated Dlp expression sufficiently and directly represses Hh and Wnt signaling in IGS cells.

### Niche-specific Dlp overexpression blocks GSC progeny differentiation primarily by elevating BMP signaling

BMP signaling elevation is known to be linked to the CB differentiation defects caused by defective Hh and Wnt signaling in IGS cells (*12*, *15*–*18*). In control germaria, BMP signaling leads to production of phosphorylated Mad (pMad), activation of Dad-lacZ reporter expression in GSCs, and represses *bam*-GFP (Fig. 2, I to K). In GSC progeny, including CBs, pMad and Dad-lacZ are turned off and *bam*-GFP is activated due to the absence of BMP signaling (Fig. 2, I to K). However, in the niche-specific Dlp-overexpressing germaria, most of the accumulated SGCs are positive for pMad and Dad-lacZ but negative for *bam*-GFP, indicating that Dlp overexpression in IGS cells elevates BMP signaling in GSC progeny, thus blocking their

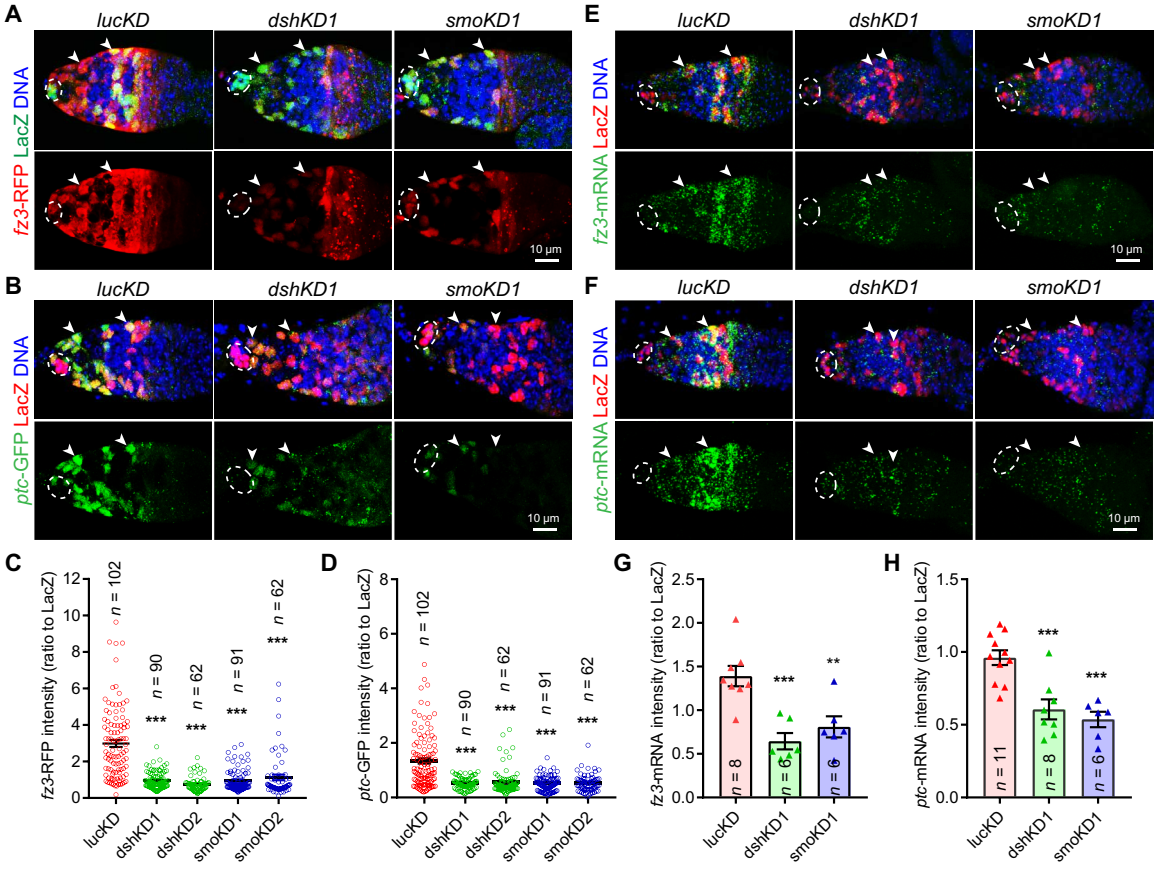


**Fig. 1. Hh and Wnt signaling are interdependent in the differentiation niche.** The germaria are labeled for PZ1444-LacZ expression to visualize IGS cells (two indicated by arrowheads) and cap cells (broken ovals), while DAPI staining identifies all nuclei. (**A** to **D**) Merged confocal images of germaria showing that the expression of both *fz3*-RFP (A) and *ptc*-GFP (B) is significantly decreased in *smoKD* and *dshKD* IGS cells 2 days after knocking down compared with the control (*lucKD*) (C and D: quantification results on *fz3*-RFP or *ptc*-GFP intensities normalized to LacZ in IGS cells, respectively; *n* = IGS cells number). (**E** to **H**) Merged FISH (green) and immunostaining (LacZ, red) confocal images showing that *fz3* (E) or *ptc* (F) mRNA expression levels are significantly reduced in *dshKD* and *smoKD* IGS cells (G and H: quantification results on *fz3* and *ptc* mRNA levels based on the fluorescence intensities normalized to LacZ, respectively; *n* = germarial number). Scale bars, 10 μm (all images at the same scale). In this study, all the quantitative data are shown as means ± SEM, whereas *P* values are determined by the two-sided Student's *t* test (***$P \leq 0.001$; **$P \leq 0.01$).

differentiation (Fig. 2, I to K). $dpp^{hr56}$ and $dpp^{hr27}$ heterozygous mutations were used previously to effectively decrease BMP signaling in the *Drosophila* ovary because *dpp* encodes a major BMP ligand in the ovary (*12*, *15*, *35*). Compared with *dlpOE*, the removal of one copy of *dpp* significantly reduces pMad level in germarium (Fig. 2L). $dpp^{hr56}$ and $dpp^{hr27}$ heterozygous mutations can significantly rescue the CB differentiation defects caused by *dlp* overexpression, but do not affect GSC numbers significantly (Fig. 2, M and N). Therefore, our experimental results demonstrate that Dlp up-regulation in IGS cells increases BMP signaling, thereby disrupting GSC progeny differentiation.

### *dlp* repression is required for the interdependence of Hh and Wnt signaling in the niche

Since Dlp is known to regulate Hh and Wnt signaling in *Drosophila* (*36*, *37*), we then determined if Dlp is required for modulating Hh and Wnt signaling in IGS cells. Although two *dlp* short hairpin RNA (shRNA) lines can efficiently knock down Dlp protein expression (fig. S3, A to D), *dlp* knockdown does not affect *fz3*-RFP and *ptc*-GFP expression in IGS cells, indicating that endogenous Dlp is dispensable for Hh and Wnt signaling activities in the differentiation niche (fig. S3, E and F). *dlp* knockdown in IGS cells can significantly rescue *fz3*-GFP expression in the *smoKD* IGS cells as well as *ptc*-GFP expression in the *smoKD* IGS cells (Fig. 3, A to C). These results indicate that Dlp repression is required for maintaining Hh and Wnt signaling independence in IGS cells.

To determine whether *dlp* up-regulation is responsible for the germ cell differentiation defects caused by defective Hh and Wnt signaling, we examined the SGC accumulation in *dlpKD dshKD* and *dlpKD smoKD* germaria. The *dlpKD lucKD* germaria contain similar GSC and CB numbers to those *lucKD* germaria, indicating that Dlp is also dispensable in IGS cells for promoting GSC progeny differentiation (Fig. 3, D and E). As expected, *dlp* knockdown in IGS cells can significantly decrease the Dlp up-regulation in IGS cells and reduce the SGC accumulation caused by *smoKD* or *dshKD* but cannot rescue the germ cell differentiation defects completely, indicating that Hh and Wnt signaling promote GSC progeny differentiation partly by repressing *dlp* expression (Fig. 3, D and E, and fig. S3, A to D). Reducing the *dlp* dosage by three independent heterozygous mutations can significantly decrease Dlp protein expression in IGS cells and also rescue the germ cell differentiation defects caused by defective Hh and Wnt signaling in IGS cells (fig. S4, A to E). This partial

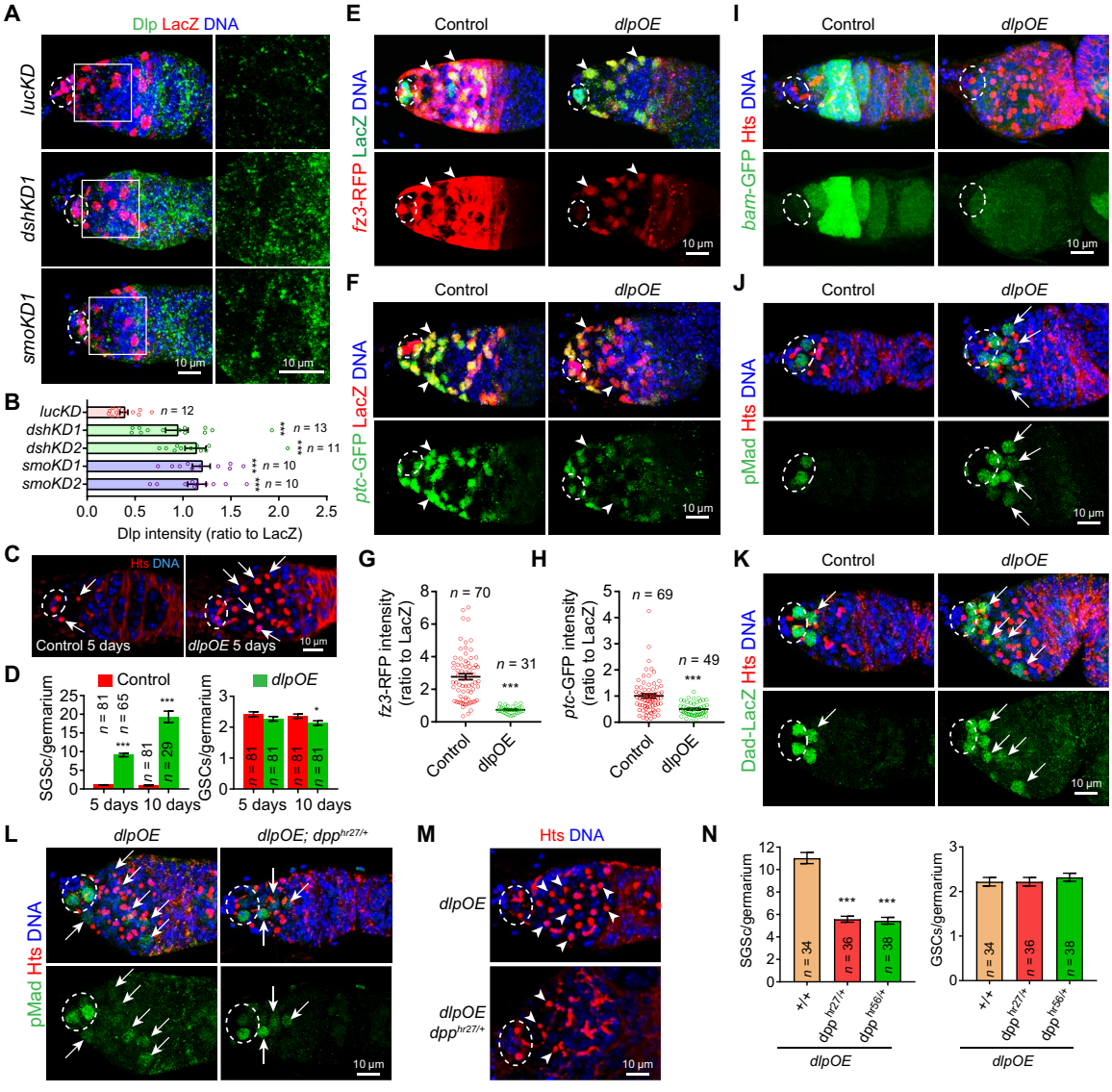


**Fig. 2. Dlp overexpression sufficiently inhibits Hh and Wnt signaling and promotes BMP signaling.** The germaria (A, E, and F) are labeled for PZ1444-LacZ to visualize IGS cells (two by arrowhead) and cap cells (broken ovals), while DAPI staining identifies all nuclei. (**A**) Merged confocal images of germaria showing that Dlp protein (green) levels are significantly up-regulated in the *dshKD1* and *smoKD1* IGS cells 2 days after knockdown (**B**: quantification results normalized to LacZ; *n* = germarial number). (**C**) *dlp* overexpression (*dlpOE*) in IGS cells causes the accumulation of significantly more spectrosome-containing undifferentiated SGCs (only two in control and four in *dlpOE* indicated by arrows) in 5- and 10-day-old germaria but have no or a little impact on GSCs (highlighted by broken ovals) (**D**: CB/SGC and GSC quantification results; *n* = germarial number). (**E** to **H**) *ptc-GFP* and *fz3-RFP* expression is drastically down-regulated in *dlpOE* IGS cells (arrowheads) 2 days after overexpression compared with the control (G and H: quantification results on *fz3*-RFP or *ptc*-GFP intensities normalized to LacZ in each IGS cell; *n* = germarial number). (**I** to **K**) Merged confocal images showing that *dlpOE* germaria accumulate more *bam-GFP*–negative, pMad-positive, and Dad-LacZ–positive SGCs (some by arrows in J and K). (**L** to **N**) Inactivating one copy of *dpp* by $dpp^{hr27/+}$ or $dpp^{hr56}$ significantly decreases both pMad-positive SGCs (L) and GSC accumulation (M) caused by *dlpOE* without any obvious effect on GSC numbers (N: CB/SGC and GSC quantification results; *n* = germarial number). Scale bars, 10 μm. (***$P \leq 0.001$; *$P \leq 0.05$).

rescue by *dlpKD* and heterozygous *dlp* mutations can be explained by the previous findings that Hh and Wnt signaling have additional important downstream targets in addition to *dlp* (*12*, *15*, *20*). *dlpKD* can only decrease the IGS cell loss caused by *dshKD* or *smoKD* 3 days, but not 5 days, after knockdown, suggesting that Hh and Wnt signaling maintain IGS cells largely independent of Dlp repression (fig. S4, F to G). Therefore, these results show that Hh and Wnt signaling–mediated *dlp* repression in IGS cells is required for their signaling interdependence and normal GSC progeny differentiation.

## Hh/Wnt signaling–mediated *dlp* repression in the niche is controlled by a regulatory region in the second intron

To further investigate how Wnt and Hh signaling repress *dlp* expression in IGS cells, we generated a series of transgenes carrying different *dlp* genomic fragments and followed with the GFP complementary DNA (cDNA) by using the pGreenRabbit (pGR) vector (Fig. 4A)(*38*). Through two rounds of genomic fragment screens, a 900–base pair (bp) genomic region (*dlp2.1.5*) in the second intron is identified to sufficiently recapitulate Dlp expression patterns in the

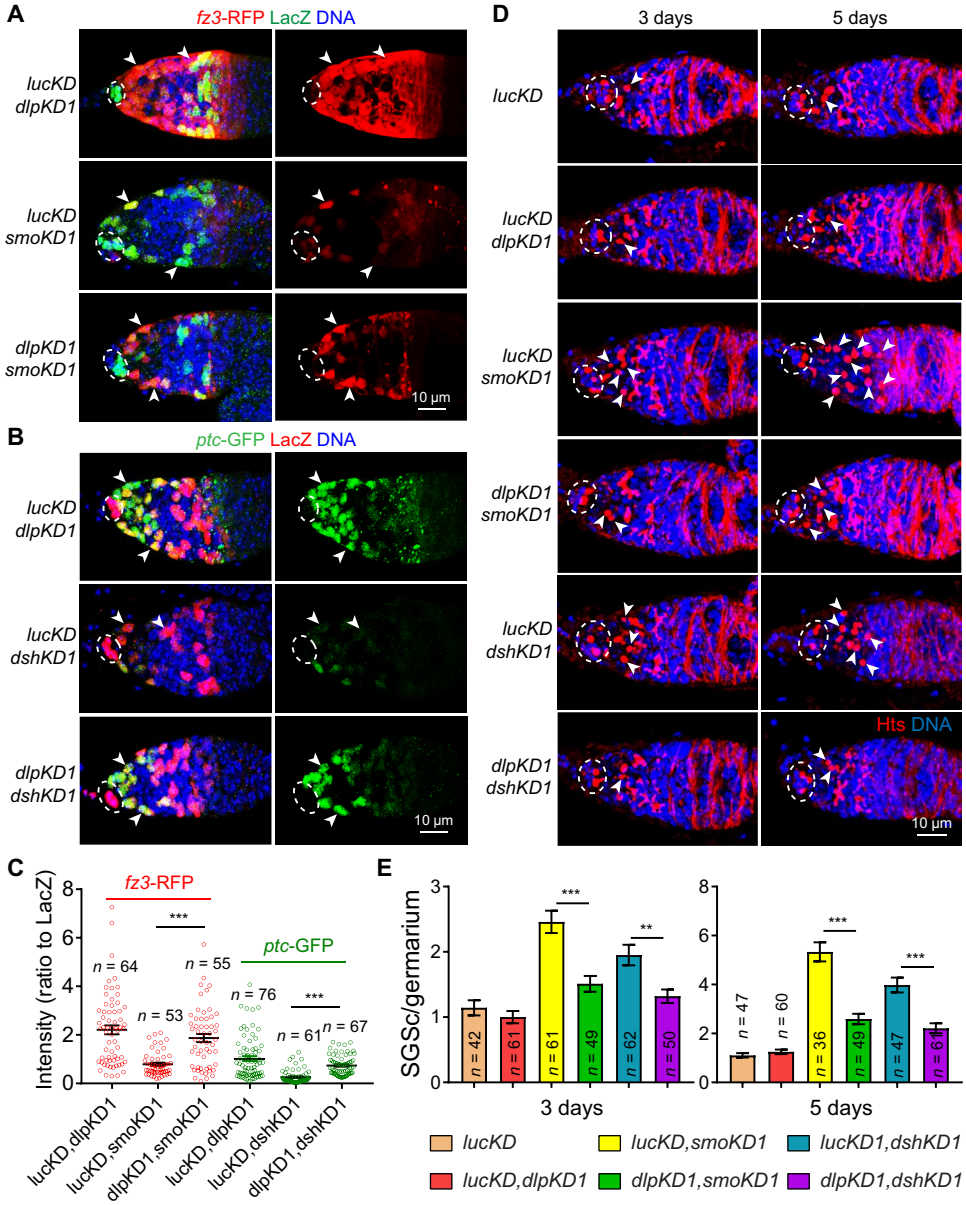


**Fig. 3. Dlp repression is responsible for Hh/Wnt signaling interdependence in IGS cells and for GSC progeny differentiation.** (**A** and **B**) *dlp* knockdown in IGS cells can significantly and drastically rescue the expression of *ptc-GFP* and *fz3-RFP* in *dshKD* and *smoKD* IGS cells (arrowheads), respectively (broken ovals highlight cap cells; **C**: quantification results on *ptc-GFP* and *fz3-RFP* fluorescence intensities normalized to *LacZ*; *n* = IGS cell numbers). (**D** and **E**) *dlp* knockdown in IGS cells can significantly decrease the accumulation of SGCs (only some of them by arrowheads) caused by *dshKD* and *smoKD* (E: CB/SGC quantification results; *n* = germarial number). Scale bars, 10 μm. (***$P \leq 0.001$; **$P \leq 0.01$).

germarium (Fig. 4B and fig. S5A). Both *dlp2.1.5*-GFP and endogenous Dlp protein show low expression in IGS cells and high expression in follicle cells (Fig. 4B). Consistent with the idea that the *dlp2.1.5* genomic region carries most, if not all, of regulatory elements for Hh/Wnt signaling–mediated repression, *dlp2.1.5*-GFP is up-regulated in both *smoKD* and *dshKD* IGS cells (Fig. 4C and fig. S5B). Transcription factors Ci and Pan function downstream of Hh and Wnt signaling, respectively, to regulate target gene expression (*39*–*41*). *dlp2.1.5-GFP* is also up-regulated in *ciKD* and *panKD* IGS cells, indicating that canonical Hh and Wnt signaling likely repress *dlp* in IGS cells via the 900-bp region (Fig. 4C and fig. S5B). *dlp* overexpression can also up-regulate *dlp2.1.5*-GFP expression, suggesting that there is a feedforward loop via Hh/Wnt signaling for the *dlp* control. These results indicate that Hh and Wnt signaling repress *dlp* transcription via a small regulatory region.

To further define individual elements in the *dlp2.1.5* region for Hh/Wnt signaling–mediated repression in IGS cells, we generated GFP reporter transgenic flies carrying nested deletions from both the ends of the 900-bp *dlp2.1.5* region with each deleting 100 bp, *dlp2.1.5* Δ*1*-GFP to *dlp2.1.5* Δ*10*-GFP (fig. S6A). Our nested deletion analyses in wild-type, *dshKD*, and *smoKD* IGS cells have yielded three pieces of important information. First, only an 800-bp continuous genomic region is sufficient for recapitulating *dlp* expression in the germarium since *dlp2.1.5* Δ*6*-GFP has the same expression

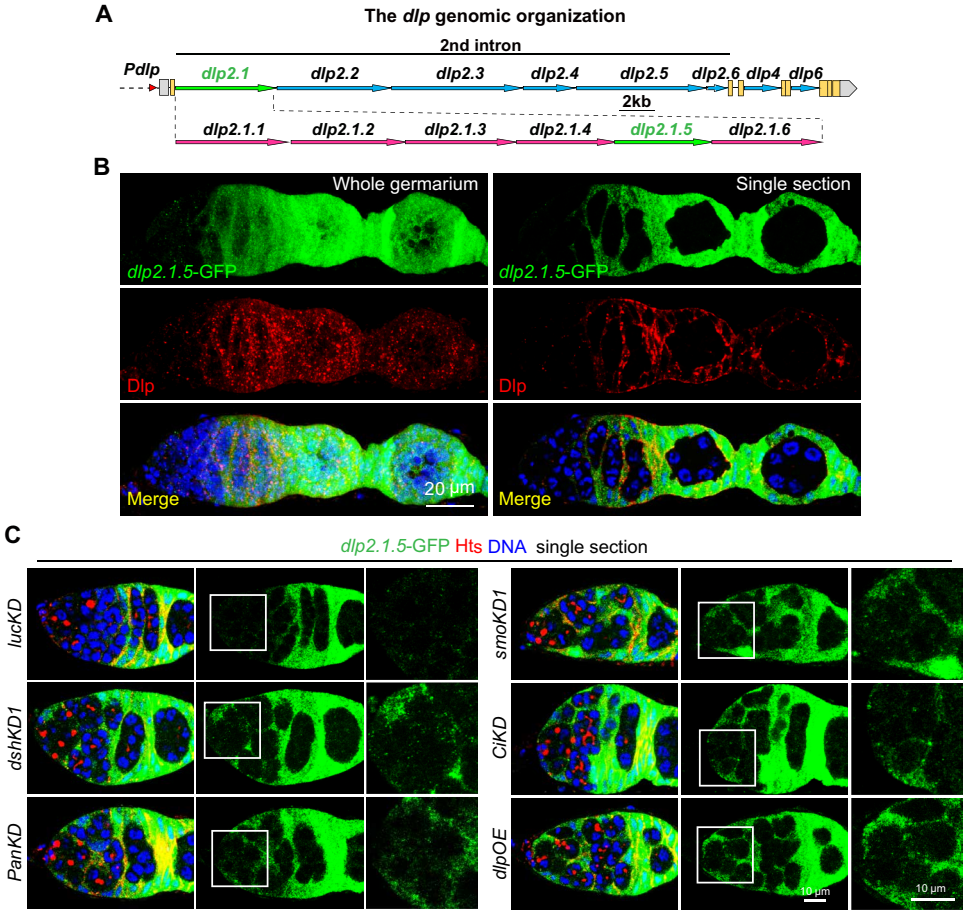


**Fig. 4. Canonical Hh and Wnt signaling repress *dlp* transcription via the *dlp2.1.5* genomic region in the second intron.** (**A**) Diagram of the *dlp* genomic regions showing *dlp2.1* and *dlp2.1.5* regions driving GFP expression, which recapitulates *dlp* mRNA and protein expression in the germarium (please see fig. S5 for details). (**B**) Immunostaining with anti-GFP (green) and anti-Dlp (red) showing *dlp2.1.5*-GFP has similar expression pattern with endogenous Dlp, which has very low level at IGS cells but high level at late-stage somatic cells. (**C**) Single confocal cross-sectional images of germaria showing that *dlp2.1.5*-GFP expression is up-regulated in *dshKD1*, *smoKD1*, *panKD*, *ciKD*, and *dlpOE* IGS cells compared with the control (*lucKD*) (anterior germarial regions highlighted by squares are shown at a high magnification). Scale bars, 20 μm in (B), 10 μm in (C).

patterns and levels as *dlp2.1.5*-GFP (fig. S6H). Second, multiple repressive elements likely scatter along the 800-bp genomic region to work synergistically for Hh/Wnt signaling–mediated *dlp* repression in IGS cells since no single 100-bp deletion in the 800-bp region alone sufficiently causes the up-regulation of the GFP reporter in IGS cells (fig. S6, B to G and I to L). Third, multiple activators in the 800-bp region are required for Dlp gene expression in follicle cells and also for defective Hh/Wnt signaling–caused Dlp up-regulation in IGS cells. On the basis of GFP expression in follicle cells, the deleted regions in *dlp2.1.5* Δ*1*, *dlp2.1.5* Δ*5*, *dlp2.1.5* Δ*7*, and *dlp2.1.5* Δ*8* are important for *dlp* expression in follicle cells and equally important for *dshKD*/*smoKD*-mediated *dlp* up-regulation. Among them, the deleted regions by *dlp2.1.5* Δ*1* and *dlp2.1.5* Δ*8* have stronger effects on *dlp* gene activation in follicle cells and also have stronger suppression effects on defective Hh/Wnt signaling–mediated *dlp* up-regulation than those deleted ones in *dlp2.1.5* Δ*5* and *dlp2.1.5* Δ*7*, suggesting that scattered repressive elements in the 800-bp region suppress *dlp* expression in IGS cells likely by antagonizing the activators. To determine whether the 800-bp-long regulatory region is required for endogenous Dlp protein expression in follicle cells, we used CRISPR-Cas9 to generate a $dlp^{\Delta 215}$ mutant deleting the region, which homozygotes are lethal likely due to its requirement for Dlp expression during early development (fig. S6N). In the $dlp^{\Delta 215}$ heterozygous mutant germarium, Dlp protein expression is deceased in follicle cells as predicted (fig. S6, O and P). Together, these results suggest that Hh/Wnt signaling–mediated *dlp* repression in the niche is accomplished through multiple cooperative repressive elements in the *dlp* regulatory region.

## Both Ci and Pan directly bind to multiple sites in the regulatory region to repress *dlp* expression in the niche

Then, we performed the electrophoretic mobility shift assay (EMSA) to determine whether Ci and Pan directly bind to multiple sites in the 800-bp region using overlapped biotin-labeled 24-bp DNA fragments and purified glutathione *S*-transferase (GST) fusion proteins with Ci and Pan DNA binding domains (Fig. 5Aand fig. S7A). Our EMSA assay has identified four strong Ci binding regions and three strong Pan binding regions in the 800-bp genomic region in addition to some weak binding sites (Fig. 5A). Two of the four Ci binding

sites, CGTGGCTGGC and GACAAGGGACT, are consistent with bioinformatic prediction, whereas only one of the three Pan binding sites, GGATACCAAAAATAGG, is predicted, suggesting that Ci and Pan are capable of binding to the previously uncharacterized new sites. Chromatin immunoprecipitation (ChIP) results have further confirmed that Ci and Pan also associate with *dlp2.1.5* region in vivo and show stronger enrichment near in vitro–identified binding regions (Fig. 5, B and C, and fig. S7B).

These Ci and Pan binding regions overlap with the activating regions, suggesting that Ci and Pan binding to the regulatory region might preclude the binding of currently uncharacterized transcription activators (Fig. 5C). Diminishing the binding activities of Ci, Pan, or both in *dlp2.1.5* by mutating the experimentally defined sites results in up-regulated GFP reporter expression in IGS cells, showing that Wnt and Hh signaling directly repress *dlp* expression in IGS cells (Fig. 5D and fig. S7, C and D). It is worth noting that *dlp2.1.5*-GFP reporter up-regulation caused by the mutated Ci or Pan binding sites is relative moderate compared with that caused by defective Hh and Wnt signaling, suggesting that Ci and Pan binding sites might overlap with the activators' binding sites in the identified *dlp* regulatory region. Together, Hh and Wnt pathway downstream transcription factors Ci and Pan can directly bind to multiple sites in the *dlp* regulatory region to repress *dlp* expression in the niche.

## Ci and Pan cooperatively recruit transcription factor Croc and H3K9 trimethylase Eggless to repress *dlp* transcription in the niche

To further investigate how Hh and Wnt signaling repress *dlp* transcription via the 800-bp genomic region in IGS cells, we then investigated how it works with Wnt signaling in IGS cells to directly repress *dlp* expression by carrying out the shRNA knockdown of transcription factors expressed in IGS cells. In the screen, crocodile (*croc*) and eggless (*egg*) were identified for their requirement in repressing *dlp2.1.5*-GFP expression in IGS cells. Knockdown of *croc* or *egg* results in the up-regulated expression of *dlp2.1.5*-GFP compared with the control (Fig. 6A). Consistent with this, *crocKD* or *eggKD* IGS cells also show increased Dlp protein expression (fig. S8, A and B). *egg* encodes an H3K9 trimethylase, which has been shown previously to be required in IGS cells for promoting GSC progeny differentiation (*9*, *42*). *croc* encodes a fork head domain–containing transcriptional factor (*43*). Consistent with the idea that Egg and Croc are involved in Dlp repression in IGS cells, knocking down *egg* or *croc* in IGS cells also leads to a significant down-regulation of Wnt and Hh signaling (fig. S8, C to F). These results suggest that Egg and Croc might be involved in Hh/Wnt signaling–mediated *dlp* repression in IGS cells.

Then, we determined whether Croc is also required in IGS cells to promote GSC progeny differentiation by directly repressing *dlp* expression. Knocking down *croc* in IGS cells by two independent shRNAs results in the accumulation of SGCs but does not affect GSC maintenance, indicating that Croc is required in the niche to promote GSC progeny differentiation (Fig. 6, B and C). In addition, our EMSA results indicate that Croc protein can also bind to two sites in the 800-bp *dlp* regulatory region (Fig. 6D and fig. S8, G and H). ChIP–quantitative polymerase chain reaction (qPCR) results have further shown that IGS–specifically expressed Croc-HA binds strongly in vivo to the in vitro–identified binding sites in the *dlp2.1.5* region (fig. S8, I and J). Notably, the Croc in vivo binding ability to the *dlp* regulatory region is significantly decreased in the *smoKD* and *dshKD* IGS cells compared with the control (Fig. 6E). Together, these results reveal that Croc binds to the *dlp* regulatory region to repress *dlp* expression in IGS cells, thereby promoting GSC progeny differentiation.

To further investigate how they work together to repress *dlp* in IGS cells, we tested whether Croc, Ci, and Pan can associate with

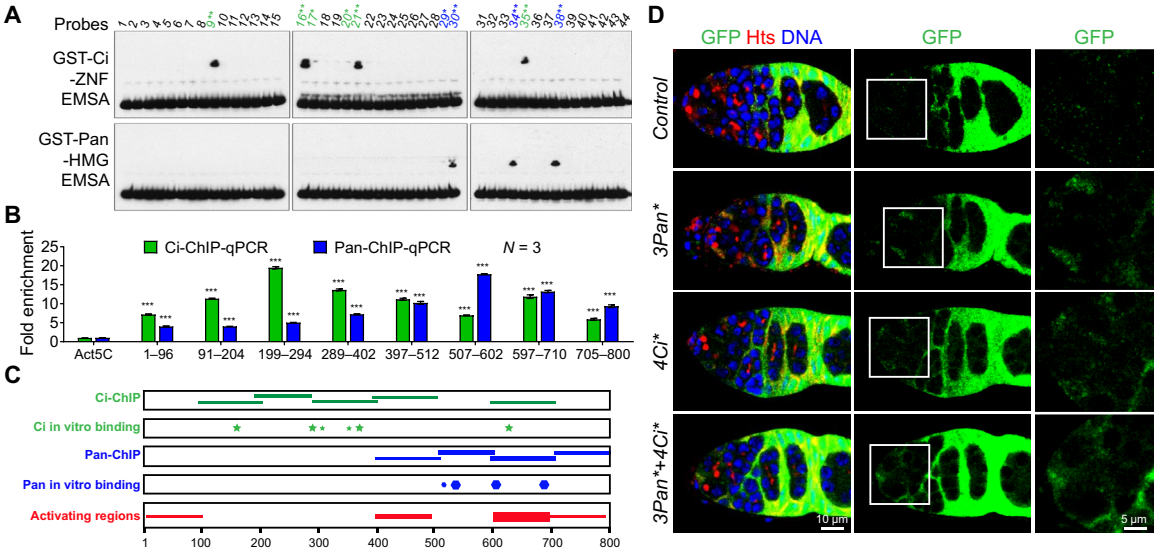


**Fig. 5. Ci and Pan bind to multiple sites in the *dlp2.1.5* genomic region for directly repressing *dlp* expression in IGS cells.** (**A**) EMSA results showing that GST-Ci-ZNF binds to four sites strongly and additional few sites weakly (green), while GST-Pan-HMG binds to three sites strongly and one site weakly (blue) (* and ** indicate weak and strong sites, respectively). (**B**) ChIP-qPCR results show that IGS-expressed Flag-Ci or Flag-Pan is associated in vivo with the 800 bp of *dlp2.1.5* (*P* values compared with background control *act5C*). Mouse IgG antibodies were used as a negative IP control. (***$P \leq 0.001$). (**C**) Summary diagram displaying Pan and Ci binding sites/regions in the *dlp2.1.5* region based on EMSA and ChIP results (A and B), as well as the expression-activating regions based on the deletion results in fig. S6. (**D**) Mutating all the strong binding sites for Pan, Ci, or both causes a moderate GFP up-regulation in IGS cells compared with *dlp2.1.5*-GFP (note: since these mutations also decrease *dlp2.1.5*-GFP expression in follicle cells, GFP expression in follicle cells are normalized to that in normal *dlp2.1.5*-GFP). Scale bars, 10 μm.

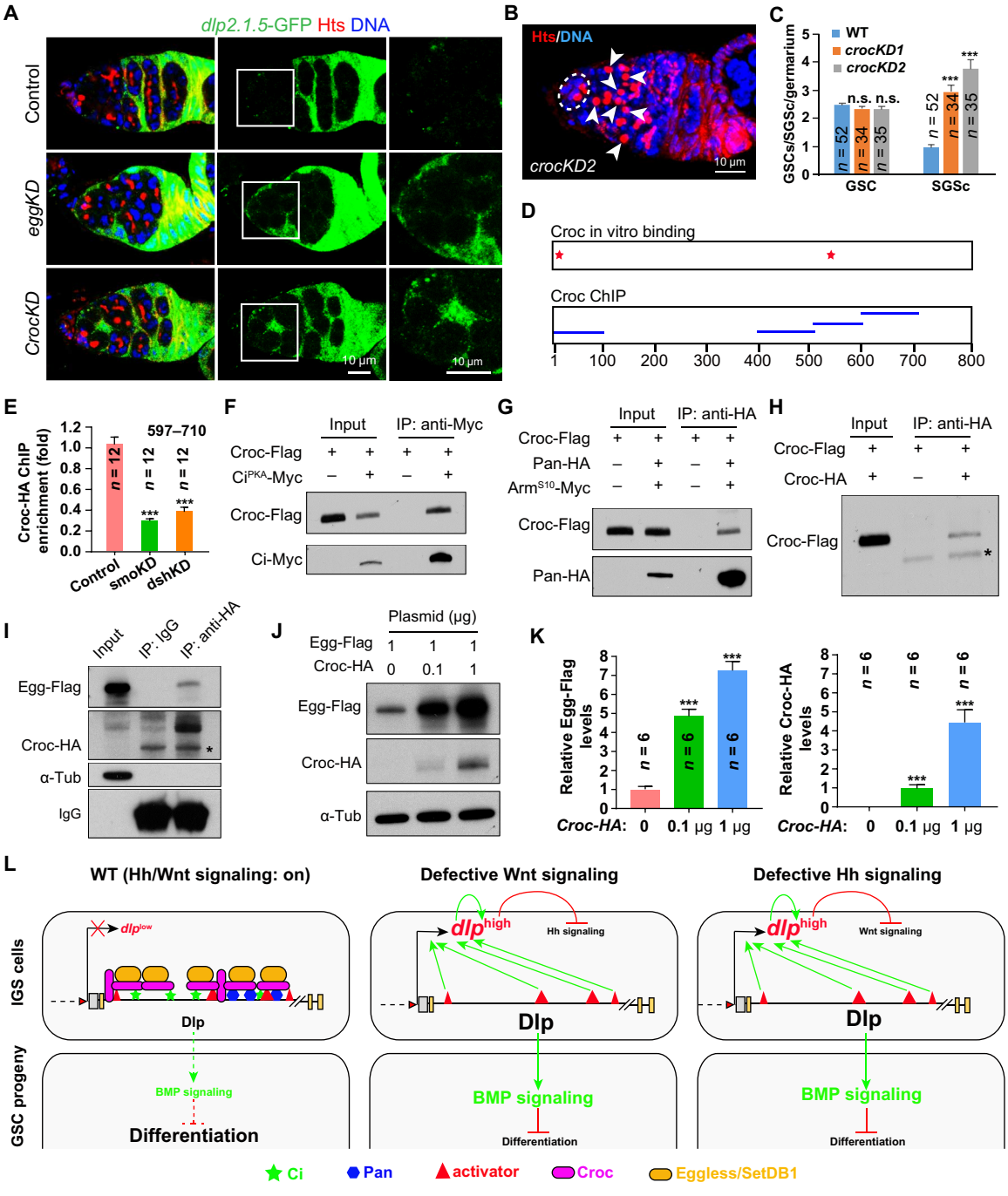


**Fig. 6. Hh/Wnt pathway downstream transcription factors Ci and Pan can recruit Croc, which subsequently recruit Eggless/SetDB1, to the *dlp2.1.5* region.** (**A**) Compared with WT, *dlp2.1.5*-GFP expression is up-regulated in *eggKD* and *crocKD* IGS cells (brackets) 5 days after knockdown. (**B** and **C**) Fourteen-day *croc* knockdown in IGS cells causes the accumulation of SGCs (arrowheads) (C: CB/SGC and GSC quantification results). n.s., no significance. (**D**) Summary diagram showing the Croc binding sites in the *dlp2.1.5* region based on EMSA and ChIP results in fig. S8 (H to J). (**E**) ChIP-qPCR results show that the binding ability of Croc to *dlp2.1.5* is significantly reduced in *smoKD* or *dshKD* IGS cells compared with WT. (**F** and **G**) In S2 cells, $Ci^{PKA}$-Myc and Pan-HA can bring down Croc-Flag. $Ci^{PKA}$ is a noncleavable active full-length Ci, whereas $Arm^{S10}$-Myc is the active Arm protein, which can bind to Pan for nuclear import in the absence of Wnt signaling. (**H**) In S2 cells, Croc-HA can bring down Croc-Flag, indicative of potential dimerization or oligomerization. (**I**) In S2 cells, Croc-HA can bring down Egg-Flag (IgG as a negative control: *, a nonspecific protein recognized by the anti-HA antibody). (**J** and **K**) Coexpression of Croc-HA can significantly increase Egg-Flag protein levels in S2 cells (empty plasmid used to normalize total transfected DNA; K: quantification results on Egg-Flag and Croc-HA levels). (**L**) Schematic diagram explaining how Hh/Wnt signaling–mediated direct Dlp repression maintains their interdependence and prevents BMP signaling, thereby promoting GSC progeny differentiation. Scale bars, 10 μm. (***$P \leq 0.001$).

each other in S2 cells. Myc-tagged stable full-length $Ci^{PKA}$-Myc, which is PKA phosphorylation resistant for preventing its cleavage (*44*), can pull down Flag-tagged Croc (Flag-Croc) (Fig. 6F). Similarly, hemagglutinin (HA)–tagged Pan (Pan-HA) can also bring down Croc-Flag in the presence of Wnt signaling activated $Arm^{S10}$, which forms a protein complex with Pan for its nuclear import (Fig. 6G) (*45*). HA-tagged Croc (Croc-HA) can also precipitate Croc-Flag, indicating that Croc proteins can dimerize or oligomerize (Fig. 6H). Flag-tagged Egg (Egg-Flag) could also be coimmunoprecipitated by Croc-HA (Fig. 6I). Croc can also significantly stabilize Egg-Flag in S2 cells in a dosage-dependent manner (Fig. 6, J and K). In summary, these results indicate that signaling-activated nuclear-localized Pan and Ci recruit Croc and, subsequently, Egg for promoting H3K9 trimethylation and, thus, blocking the access of the transcriptional activators to the *dlp2.1.5* region and preventing dlp transcription in IGS cells.

## DISCUSSION

Although Shh and Wnt signaling work synergistically to promote neural stem cell proliferation/differentiation in the mouse developing brain as well as cell proliferation in human medulloblastoma, the underlying mechanisms remain missing (*46*, *47*). In addition, both Hh and Wnt signaling have also been shown to be required in the niche to promote GSC progeny differentiation in the *Drosophila* ovary by repressing BMP signaling, but the cooperative mechanisms are also not understood as well (*15*, *17*–*19*). In this study, we show that Hh and Wnt signaling sustain each other in the niche by directly repressing Dlp expression through Ci/Pan-recruited transcription factor Croc and H3K9 trimethylase Egg, and such repression is critical for preventing BMP signaling and, thus, promoting GSC progeny differentiations (Fig. 6L).

### Dlp repression–mediated interdependence in the niche is a novel mechanism for Hh and Wnt signaling cooperation

The cooperative and antagonistic relationships between Hh and Wnt signaling have been well established in normal developmental contexts and various human tumors. The antagonistic relationship between Hh and Wnt signaling is often accomplished through intrinsic signal transducers, target genes, and secreted inhibitors (*48*, *49*). In *Drosophila*, Wg and Hh often regulate the same developmental processes synergistically through regulating each other's expression (*50*, *51*). However, the molecular mechanisms underlying Hh and Wnt signaling synergistic relationships remain largely unknown. Our findings have revealed a new Hh and Wnt signaling interdependent relationship maintained by a novel Dlp-mediated mechanism.

This study has provided the convincing experimental evidence supporting the Dlp repression–mediated Hh and Wnt signaling interdependence. First, Wnt and Hh signaling are required for each other to sustain their signaling activities in the niche. Second, Hh and Wnt signaling are required in the niche to directly repress Dlp expression since *dlp* mRNA and protein are significantly up-regulated in the Hh/Wnt signaling–defective niche. Third, niche-specific Dlp overexpression eliminates Hh/Wnt signaling in the niche. Fourth, Dlp overexpression can also further induce its own transcription, likely through inactivating Hh and Wnt signaling, suggesting that there is a feedforward loop for *dlp* regulation in the niche. Last, Dlp repression in the niche is critical for the interdependence of Hh and Wnt signaling. Together, our findings demonstrate that Hh/Wnt signaling–mediated *dlp* repression is essential for maintaining the Hh/Wnt signaling interdependence in the niche (Fig. 6L). Although this study has revealed a novel mode for Hh/Wnt signaling cooperation as well as a novel mechanism mediating such cooperation, many important questions remain to be answered, such as how Dlp up-regulation inhibits Hh and Wnt signaling mechanistically in the niche and whether such regulatory mechanism operates in other developmental contexts and some diseased conditions.

### Hh/Wnt signaling–mediated Dlp repression represents a new mechanism for the differentiation niche to prevent BMP signaling

BMP signaling activated by GSC niche-secreted Dpp is necessary and sufficient for maintaining GSC self-renewal by repressing differentiation (*5*). IGS cells function as a niche for promoting GSC progeny differentiation partly by preventing BMP signaling (*3*). Recent several studies have shown that Hh and Wnt signaling are required in IGS cells to promote GSC progeny differentiation partly by preventing BMP signaling via multiple mechanisms. Hh signaling functions in IGS cells to repress *dpp* expression and antagonize Hippo signaling, thereby preventing BMP signaling (*12*, *20*). Wnt signaling is required in IGS cells to prevent BMP signaling activities in GSC by maintaining Tkv expression, IGS cellular processes, and the redox state, as well as by repressing *dpp* expression (*15*–*18*). On the basis of our data, we propose a model that Hh and Wnt signaling function in IGS cells to prevent BMP signaling in GSC progeny by repressing *dlp* expression (Fig. 6L).

This study has provided several pieces of experimental evidence demonstrating that Hh/Wnt signaling–mediated Dlp repression in IGS cells is essential for preventing BMP signaling and promoting GSC progeny differentiation. Dlp up-regulation in IGS cells causes BMP signaling elevation in GSC progeny as well as severe differentiation defects. In addition, decreasing BMP signaling by *dpp* mutations can significantly and drastically rescue the differentiation defects caused by Dlp overexpression in the niche. Furthermore, *dlp* knockdown in the niche can significantly rescue the GSC differentiation defects caused by defective Hh or Wnt signaling. Consistent with our findings, Dlp has been suggested to promote BMP signaling by increasing BMP concentration at the cell surface or functioning as a BMP coreceptor in *Drosophila* (*24*). It will be of great interest to investigate how Dlp mechanistically promotes BMP signaling in the differentiation niche.

### Hh and Wnt signaling use a novel mechanism for repressing *dlp* expression in the niche

Wnt signaling has been shown to directly repress the transcription of *dpp* in the leg imaginal disc by recruiting the Pan/Arm/Brinker complex to canonical T cell factor (TCF) binding sites and the transcription of *Ugt36Bc* in the hemocyte by recruiting the TCF/Pan complex to uncanonical TCF binding sites (*52*, *53*). Hh signaling has only been reported to directly repress *tkv* expression in *Drosophila* wing imaginal disc via the full-length Ci, but the underlying mechanism remains unclear (*54*). This study shows that Hh and Wnt signaling can directly repress *dlp* expression by recruiting the Croc-Egg protein complex to TCF and Ci binding sites in the *dlp* regulatory region (Fig. 6L).

In this study, we have revealed that Hh and Wnt signaling downstream transcription factors Ci and Pan bind to multiple sites of a *dlp* regulatory region to antagonize activators, thereby repressing *dlp* expression. The 800-bp-long regulatory region in the second intron

of *dlp* (*dlp2.1.5*) sufficiently recapitulates the expression pattern of Dlp protein in the *Drosophila* ovary based on the GFP reporters containing different *dlp* genomic fragments. This region carries all the necessary elements capable of responding to Hh/Wnt signaling properly. Further analysis on 100-bp-long nested deletions has shown that four deletions decease *dlp2.1.5*-GFP up-regulation in Hh/Wnt signaling–defective IGS cells, but no single deletion up-regulates *dlp2.1.5*-GFP expression, suggesting that multiple repressive elements in the regulatory region are required for repressing *dlp* expression in the niche, likely by antagonizing the function of the activating elements. Consistently, both Pan and Ci can bind to multiple sites of the identified regulatory region in vitro and in vivo. These Pan and Ci binding sites are also overlapped with the regions containing the activating elements. Last, mutating either Pan binding sites or Ci binding sites in the *dlp* regulatory region causes the moderate up-regulation of *dlp2.1.5*-GFP in the niche compared with its strong up-regulation in the Hh/Wnt signaling–defective niche. Curiously, these mutations also decrease the expression of *dlp2.1.5*-GFP in follicle cell progenitors. Together, these findings lead us to propose a model that on Hh and Wnt signaling activation, Ci and Pan bind the regulatory region of *dlp* and repress its expression in the niche partly by preventing the recruitment of unknown transcriptional activators.

This study has further suggested that Ci and Pan sequentially recruit Croc and Egg/H3K9 to the *dlp* regulatory region to maintain transcriptional repressive mark H3K9me3 and, thus, prevent *dlp* transcription. Both Croc and Egg are required in the niche for repressing *dlp* expression and for promoting GSC progeny differentiation. *egg* is an H3K9 trimethylase required in the niche for promoting GSC progeny differentiation (*9*), whereas Croc is a known fork head domain–containing transcriptional factor (*43*). Croc can also directly bind to two independent sites in the same *dlp* regulatory region in an Hh/Wnt signaling–dependent manner in vivo, and one of them is also in close proximity to Pan and Ci binding sites. In S2 cells, both Pan and Ci are associated with Croc, which is also associated with and stabilizes Egg. On the basis of these results, we propose that on Hh and Wnt signaling activation, Ci and Pan recruit the Croc-Egg protein complex to the *dlp* regulatory region to directly repress *dlp* expression, likely through maintaining H3K9me3 (Fig. 6L).

Among six Dlp-related mammalian GPC proteins, GPC4 and GPC6 can functionally replace Dlp to promote Hh signaling in *Drosophila*, whereas GPC2, GPC3, and GPC5 are inhibitory on Hh signaling when overexpressed (*26*). In mammals, Dlp homologs GPC3 and GPC5 can inhibit and activate Hh signaling, respectively (*25*, *55*), whereas GPC3 and GPC4 can promote and repress canonical Wnt signaling (*27*, *56*), indicating that the ability of Dlp to repress and activate Hh and Wnt signaling is conserved from *Drosophila* to mammals. These findings raise the interesting possibility that the Dlp-mediated feedback control of Hh and Wnt signaling interdependence might also help elucidate their cooperative mechanisms in mammalian development, stem cell regulation, and cancer.

## MATERIALS AND METHODS

### *Drosophila melanogaster* stocks

The following *Drosophila* stocks used in this study are described in FlyBase, unless specified: *c587*, *tubulin-gal80$^{ts}$*, *smoRNAi* (BL27037 and BL62987) (*12*), *dshRNAi* (BL31306 and BL31307), *ciRNAi* (BL64928), *PanRNAi* (BL40848), *dlpRNAi* (BL34089 and BL34091), *crocRNAi* (BL27071 and BL34647), *eggRNAi* (BL32445 and BL34803), *tkvRNAi* (BL40937 and BL57303), *lucRNAi* (BL31603), *bamGFP*, *Dad-lacZ*, *ptc-GFP* (*29*, *30*), *fz3-RFP* (*28*, *30*), *UAS-CD8::GFP*, *UAS-dlp*, *UAS-Croc-3*×HA (FlyORF: F000139), *dlp$^{MI04217}$*, *dlp$^{MI09937}$*, and *dlp$^{MI10064}$*. *Drosophila* strains were maintained and crossed at room temperature on standard cornmeal/molasses/agar media unless specified. To maximize the RNAi-mediated knockdown effect, newly eclosed flies at room temperature were cultured at 29°C for the specified days before phenotypic analysis.

### Plasmid construction

The Invitrogen Gateway Technology was used to make the constructs for expressing Flag-tagged Ci, Flag-tagged Pan, Flag-tagged Dlp, HA-tagged Wnt2, HA-tagged Wnt4, Flag-tagged Egg, Flag-tagged Croc, and HA-tagged Croc in S2 cells for co-IP experiments or for making transgenic flies. The coding sequences for *ci*, *pan*, *dlp*, *wnt2*, *wnt4*, *egg*, and *croc* were amplified from *Drosophila* ovarian cDNAs using PCR. The *arm$^{S10}$* sequence was amplified from the genomic DNA from the *UAS-arm$^{S10}$* transgenic strain (BL4782). All the PCR products were cloned into the pENTR-TOPO cloning vector and were completely sequenced. These pENTR vectors were subsequently recombined into Flag-, Myc-, or HA-tagged destination vectors (pAWF, pAWH, pAWM, and pTWF) by using LR Clonase (Invitrogen). *UAS-Myc-Ci$^{PKA}$* was a gift from J. Jiang (*57*). Since Dlp protein undergoes internal proteolytic cleavage, the 3× Flag tag was inserted after the 18th amino acid residue, and the termination codon was added to the reverse primer to skip the Flag tag in the pAWF destination vector. The GST fusion proteins with Ci (GST-Ci), Pan (GST-Pan), or Croc (GST-Croc) were constructed by cloning the DNA fragments encoding five Ci ZnF_C2H2 domains, the Pan HMG domain, or the Croc FH domain into the Eco RI and Xho I sites of pGEX4T1, respectively.

### Immunostaining

Ovaries were dissected, fixed, and stained according to the method described previously (*58*, *59*). The following antibodies were used in this study: mouse monoclonal anti-Dlp antibody [1:10; Developmental Studies Hybridoma Bank (DSHB)], mouse monoclonal anti-Hts antibody (1:50; 1B1, DSHB), rabbit polyclonal anti-β-galactosidase (LacZ) antibody (1:500; MP Biomedical, no. 08559761), mouse monoclonal anti-β-galactosidase (LacZ) antibody (1:50; JIE7, DSHB), rabbit monoclonal anti-Smad3 antibody (pS423/pS425) (1:200; Epitomics, ab52903), rabbit polyclonal anti-RFP (1:1000; Rockland, no. 600-401-379), and chicken polyclonal anti-GFP antibody (1:500; Invitrogen, no. A10262).

### S2 cell transfection and co-IP

S2 cells were grown at 25°C in the HyClone SFX-Insect Cell Culture Media (Thermo Fisher Scientific). Transfections were performed using the X-treme GENE HP (6366546001, Roche) transfection reagent according to the manufacturer's instructions. For co-IP experiments in S2 cells, 12 ml of S2 cells was transfected by indicated plasmids. The transfected S2 cells were then lysed with 800 μl of ice-cold lysis buffer [50 mM tris-HCl (pH 7.5), 150 mM NaCl, 0.5% Triton X-100, 1 mM EDTA, and a mixture of protease inhibitors]. The supernatant of the lysate was incubated with 2 μg of mouse anti-HA, mouse anti-Flag, or mouse anti-Myc. Protein A/G agarose (40 μl; sc-2003; Santa Cruz Biotechnology), which was prewashed in 5% bovine serum albumin at 4°C for 1 hour, was added to the supernatant. The supernatant-antibody-agarose mix was incubated overnight

at 4°C. After six washes with the lysis buffer, the bound complexes were eluted with 2× SDS sample buffer and subjected to SDS–polyacrylamide gel electrophoresis and immunoblotting. Mouse anti–α-tubulin (T9026, Sigma-Aldrich; 1:10000), mouse anti-Flag (F1804, Sigma-Aldrich; 1:2000), mouse anti-Myc (M4439, Sigma-Aldrich; 1:2000), or mouse anti-HA (H3663, Sigma-Aldrich; 1:2000) antibodies were used for immunoblotting. To avoid the interference of immunoglobulin G (IgG) heavy chain (~55 kDa), horseradish peroxidase–goat anti-mouse IgG light chain secondary antibodies were used. Inputs were extracted before IP.

### Construction of the *GFP* reporters for *dlp*

To construct the *dlp* reporter plasmids, we then used the following primer pairs carrying either Xba I or Kpn I at the 5′ end to amplify the DNA fragments from the *Drosophil*a genomic DNA, which were confirmed by complete sequencing and then cloned into the pGR vector:

*dlp* promotor: agtctctagactttcgatagtgtggaccttcctt; aagtggtaccgtatgtacagtgtcactaggctat.

*dlp2.1*: cgactctagagtatgtccgatattatataccaat; cgacggtaccgcatttatatactttgttgtagttg.

*dlp2.2*: cgactctagataataatagtaggca; cgacggtaccttgccacattccaccttagctatt.

*dlp2.3*: aaggtctagaaatggggctagctta; cgacggtaccaagggagaacggagccaaactcca.

*dlp2.4*: ttggtctagaacaagttttcgaatga; cgacggtaccatgtggacataatcgagcataa.

*dlp2.5*: attttctagaatgtatttctggagt; cgacggtaccagactctgatacgcatacaggata.

*dlp2.6*: agtctctagatggtgccacactcca; aagtggtaccattttgttaatctct.

*dlp4*: agtctctagagtgagtagtagtctgcgaaatcca; aagtggtacctggaaaataagattaaatcggtg.

*dlp6*: agtctctagagtgagatctacagcggaataatt; aagtggtacctgcaatgaattaatttgagagtt.

*dlp2.1.1*: cgactctagagtatgtccgatattatataccaat; cgacggtacctcacgcagttcacgccaacgatgct.

*dlp2.1.2*: cgactctagaagcatcgttggcgtgaactgcgtga; cgacggtaccaatctgttattaaaatttgtccta.

*dlp2.1.3*: cgactctagataggacaaattttaataacagatt; cgacggtaccagttgcgatctacaaagccaatct.

*dlp2.1.4*: cgactctagaagattggctttgtagatcgcaact; cgacggtaccacaatggtcaacaattgcagaagt.

*dlp2.1.5*: cgactctagaacttctgcaattgttgaccattgt; cgacggtacctggccacgtttgacctgctcgaga.

*dlp2.1.6*: cgactctagatctcgagcaggtcaaacgtggcca; cgacggtaccgcatttatatactttgttgtagttg.

*dlp2.1.5*Δ1: gctctagactgtctggtgtttgtttatgagg; cgacggtaccgcatttatatactttgttgtagttg.

*dlp2.1.5*Δ*2*: gctctagaaaaacttatgaagctttttttaatatgattagcaaac; cgacggtaccgcatttataactttgttgtagttg.

*dlp2.1.5*Δ*3*: gctctagacatctggtaaaccgaaagctt; cgacggtaccgcatttatatactttgttgtagttg.

*dlp2.1.5*Δ*4*: gctctagatacaattactcagttcctagggg; cgacggtaccgcatttatatactttgttgtagttg.

*dlp2.1.5*Δ5: gctctagacggtgctgggattccaga; cgacggtaccgcatttataactttgttgtagttg.

*dlp2.1.5*Δ*6*: cgactctagaacttctgcaattgttgaccattgt; agacggtacctgccggcaattaagtcgt.

*dlp2.1.5*Δ*7*: cgactctagaacttctgcaattgttgaccattgt; agacggtacctccacaggattcattcttagaaaatttgc.

*dlp2.1.5*Δ*8*: cgactctagaacttctgcaattgttgaccattgt; agacggtacctcagctaattacgcgaaattgc.

*dlp2.1.5*Δ*9*: cgactctagaacttctgcaattgttgaccattgt; agacggtaccatcactggatcagatagcacc.

*dlp2.1.5*Δ*10*: cgactctagaacttctgcaattgttgaccattgt; agacggtaccatggcatattagggggcg.

To make *dlp2.1.5*(*3Pan**)-*GFP* transgenes, the three identified Pan binding sites in gcccacaaagtcaacacttgctga, ctgacgatgctgacagaaatggga, and tcagcaaattttctaagaatgaat were mutated to gcccacaaagtttacacttgctga, ctgacgatgcaaacagaaatggga, and tttgcaaattttctaagaatgaat, respectively. To make *dlp2.1.5*(*4 Ci**)-*GFP* transgenes, the four identified Ci binding sites in cgtttatcacgggggcttttcgca, actgacaacccactaaactagatc, agcaaactctttcacgcgatctcg, and atgggatctcccagccggcagcca were mutated to cgtttatcacggggttttttgca, actaacaaaacactaaactagatc, agcaaactctttcacgttatcttg, and atggaatctaacagccggcagcca, respectively. For the *dlp2.1.5*(*3Pan**+*4Ci**)-*GFP* reporter, all of the seven binding sites were mutated. All the constructs were inserted into the *attp40* site on the second chromosome using *PhiC31* integrase–mediated transgenesis by Rainbow Transgenic Flies Inc.

### Generation of the *dlp2.1.5* deletion mutant

The $dlp^{\Delta 215}$ (deleting first 800 bp in *dlp2.1.5* region) mutant was designed and generated by Rainbow Transgenic Flies Inc. using the CRISPR-Cas9 technology. The following guide RNAs (gRNAs) were used: gRNA1 target, 5-gaattgttgaccattgtatgg; gRNA2 target, 5-ggccaacgacttaattgccgg. Mutants were confirmed by PCR and sequencing. Primers used for PCR identification were 5-gcaaccaccgcatgactatta and 5-gatgggaaagagacagcaact.

### Purification of bacterially expressed GST, GST-Ci, GST-Pan fusion proteins and in vitro DNA binding assays

The *Escherichia coli* bacteria strains were transfected with GST, GST-Ci-ZNF, GST-Pan-HMG, or GST-Croc-FH plasmid, and the culture for each bacteria strain was grown to the density of $OD_{650}$ (optical density at 650 nm) = 0.1 to 0.25. The expression of the fusion proteins was then induced by the addition of 0.2 mM isopropyl-β-D-thiogalactopyranoside for overnight at 16°C. The cells were then harvested and lysed with B-PER with Enzymes Bacterial Protein Extraction Kit (90079, Thermo Fisher Scientific), and the proteins were purified with glutathione agarose (16100, Thermo Fisher Scientific). The in vitro DNA-protein binding assay was performed according to the LightShift Chemiluminescent EMSA Kit (20148, Thermo Fisher Scientific). Glycerol (4.35%), magnesium chloride (5 mM), poly(dI-dC) (50 ng/ml), and NP-40 (0.05%) were included in the binding reaction. For each 20 μl of binding assay, 0.1 nM biotin-labeled probe (synthesized by Integrated DNA Technologies) and 10 μg of purified GST protein or GST fusion protein were used.

### ChIP and PCR or qPCR

ChIP was performed essentially as described by the Pierce Agarose ChIP Kit (26156, Thermo Fisher Scientific). For each genotype, 200 pairs of ovaries were dissected and then digested with type II collagenase (50D11833; Worthington). The late-stage egg chambers and mature eggs were filtered and removed. Primers used for regular PCR are as follows:

1–96: acttctgcaattgttgaccattgt; tcctactcgtttatataccccgcc.

91–204: gtaggagttgctgtctggtgtttg; ttttagattttatatacccaaagc.

199–294: ctaaaacttatgaagctttttta; gatctagtttagtgggttgtcagt.

289–402: tagatcacctaacatctggtaaac; taatggcatattagggggcgagat.

397–512: ccattacaattactcagttcctag; atcccagcaccgatcactggatca.

507–602: tgggattccagacattttgcccac; cgtcagctaattacgcgaaattgc.
597–710: gcaatttcgcgtaattagctgacg; tcatccgcgatccacaggattcat.
705–800: ggatgattcaagttggattcgagt; tgccggcaattaagtcgttggccc.

For comparing the binding affinities of Croc to the *dlp* regulatory region between *WT*, *smoKD*, and *dshKD* IGS cells, qPCR was performed using PerfeCTa SYBR Green FastMix (Quantabio, no. 022048) according to the manufacturer's recommendations and analyzed using the $2^{-\Delta\Delta CT}$ method. Sequences of primers are tgggattccagacattttgcccac and gtcagctaattacgcgaaattgc. *actin5C* was used as internal control (primers: atcgggatggtcttgattctg and actccaaacttccaccactc).

### Hybrid chain reaction combined with immunostaining

To assess the expression level of *fz3*, *ptc*, and *dlp* mRNA in control, *smoKD*, and *dshKD* IGS cells, we performed FISH on ovaries, which are immunostained for PZ1444-LacZ (labeling IGS cells). Hybridization chain reaction (HCR) was used to achieve high-sensitivity FISH for quantification. Probe sets against *fz3*-mRNA (lot: PDR091), *ptc*-mRNA (lot: PDR092), or *dlp*-mRNA (lot: PDR093) were ordered from Molecular Instruments Inc. Immunostaining ovaries using anti-LacZ antibodies was performed according to the previous publication before in situ hybridization (*60*). Then, standard steps following HCR v3.0 protocol for whole-mount fruit fly embryos were applied. At the end of HCR in situ hybridization, 4′,6-diamidino-2-phenylindole (DAPI) was added at 1 μg/μl for 10 min in 5× SSCT (1X saline-sodium citrate buffer with 0.1% Triton X-100) buffer to the ovaries and then washed 15 min in 5× SSCT for four times. Last, the ovaries were mounted, and images were captured according to the regular immunostaining protocol.

### Imaging, quantification, and statistical analysis

GSCs and CBs were quantified under the fluorescence microscope according to the method described previously (*58*). The germaria were imaged by the Leica SP5 confocal microscope, and the images with all sections were merged unless specified. For confocal images, fluorescence intensities for the highlighted areas of interest were quantified using the Leica software, and the mean values of fluorescence intensities and internal controls were collected. The ratio of mean values of intensities of interest to internal controls was calculated and subjected for statistical analysis using Student's *t* test in Microsoft Excel or GraphPad Prism 7. For *fz3*-RFP and *ptc*-GFP reporters, the intensity of single IGS cell nuclear was measured, because these reporters express nuclear located RFP or GFP. For other staining, intensity of IGS cell region in each germarium was measured. All bar graphs are represented as means ± standard error and with individual value (***$P \leq 0.001$; **$P \leq 0.01$; *$P \leq 0.05$; n.s., no significance).

## SUPPLEMENTARY MATERIALS

Supplementary material for this article is available at http://advances.sciencemag.org/cgi/content/full/6/20/eaaz0480/DC1

View/request a protocol for this paper from *Bio-protocol*.

## REFERENCES AND NOTES


1. L. Li, T. Xie, Stem cell niche: Structure and function. *Annu. Rev. Cell Dev. Biol.* **21**, 605–631 (2005).
2. S. J. Morrison, A. C. Spradling, Stem cells and niches: Mechanisms that promote stem cell maintenance throughout life. *Cell* **132**, 598–611 (2008).
3. D. Kirilly, S. Wang, T. Xie, Self-maintained escort cells form a germline stem cell differentiation niche. *Development* **138**, 5087–5097 (2011).
4. T. DeFalco, S. J. Potter, A. V. Williams, B. Waller, M. J. Kan, B. Capel, Macrophages contribute to the spermatogonial niche in the adult testis. *Cell Rep.* **12**, 1107–1119 (2015).
5. T. Xie, Control of germline stem cell self-renewal and differentiation in the *Drosophila* ovary: Concerted actions of niche signals and intrinsic factors. *WIREs Dev. Biol.* **2**, 261–273 (2013).
6. A. Spradling, M. T. Fuller, R. E. Braun, S. Yoshida, Germline stem cells. *Cold Spring Harb. Perspect. Biol.* **3**, a002642 (2011).
7. T. Xie, A. C. Spradling, A niche maintaining germ line stem cells in the *Drosophila* ovary. *Science* **290**, 328–330 (2000).
8. X. Song, G. B. Call, D. Kirilly, T. Xie, Notch signaling controls germline stem cell niche formation in the *Drosophila* ovary. *Development* **134**, 1071–1080 (2007).
9. X. Wang, L. Pan, S. Wang, J. Zhou, W. McDowell, J. Park, J. Haug, K. Staehling, H. Tang, T. Xie, Histone H3K9 trimethylase Eggless controls germline stem cell maintenance and differentiation. *PLOS Genet.* **7**, e1002426 (2011).
10. E. J. Ward, H. R. Shcherbata, S. H. Reynolds, K. A. Fischer, S. D. Hatfield, H. Ruohola-Baker, Stem cells signal to the niche through the Notch pathway in the *Drosophila* ovary. *Curr. Biol.* **16**, 2352–2358 (2006).
11. L. X. Morris, A. C. Spradling, Long-term live imaging provides new insight into stem cell regulation and germline-soma coordination in the *Drosophila* ovary. *Development* **138**, 2207–2215 (2011).
12. T. Lu, S. Wang, Y. Gao, Y. Mao, Z. Yang, L. Liu, X. Song, J. Ni, T. Xie, COP9-Hedgehog axis regulates the function of the germline stem cell progeny differentiation niche in the *Drosophila* ovary. *Development* **142**, 4242–4252 (2015).
13. T. U. Banisch, I. Maimon, T. Dadosh, L. Gilboa, Escort cells generate a dynamic compartment for germline stem cell differentiation via combined Stat and Erk signalling. *Development* **144**, 1937–1947 (2017).
14. M. Liu, T. M. Lim, Y. Cai, The *Drosophila* female germline stem cell lineage acts to spatially restrict DPP function within the niche. *Sci. Signal.* **3**, ra57 (2010).
15. S. Wang, Y. Gao, X. Song, X. Ma, X. Zhu, Y. Mao, Z. Yang, J. Ni, H. Li, K. E. Malanowski, P. Anoja, J. Park, J. Haug, T. Xie, Wnt signaling-mediated redox regulation maintains the germ line stem cell differentiation niche. *eLife* **4**, e08174 (2015).
16. M. Upadhyay, Y. Martino Cortez, S. Wong-Deyrup, L. Tavares, S. Schowalter, P. Flora, C. Hill, M. A. Nasrallah, S. Chittur, P. Rangan, Transposon dysregulation modulates dWnt4 signaling to control germline stem cell differentiation in drosophila. *PLOS Genet.* **12**, e1005918 (2016).
17. V. I. Mottier-Pavie, V. Palacios, S. Eliazer, S. Scoggin, M. Buszczak, The Wnt pathway limits BMP signaling outside of the germline stem cell niche in *Drosophila* ovaries. *Dev. Biol.* **417**, 50–62 (2016).
18. L. Luo, H. Wang, C. Fan, S. Liu, Y. Cai, Wnt ligands regulate Tkv expression to constrain Dpp activity in the *Drosophila* ovarian stem cell niche. *J. Cell Biol.* **209**, 595–608 (2015).
19. N. Hamada-Kawaguchi, B. F. Nore, Y. Kuwada, C. I. Smith, D. Yamamoto, Btk29A promotes Wnt4 signaling in the niche to terminate germ cell proliferation in *Drosophila*. *Science* **343**, 294–297 (2014).
20. C. Li, L. Kan, Y. Chen, X. Zheng, W. Li, W. Zhang, L. Cao, X. Lin, S. Ji, S. Huang, G. Zhang, X. Liu, Y. Tao, S. Wu, D. Chen, Ci antagonizes Hippo signaling in the somatic cells of the ovary to drive germline stem cell differentiation. *Cell Res.* **25**, 1152–1170 (2015).
21. I. Maimon, M. Popliker, L. Gilboa, Without children is required for Stat-mediated zfh1 transcription and for germline stem cell differentiation. *Development* **141**, 2602–2610 (2014).
22. T. Akiyama, K. Kamimura, C. Firkus, S. Takeo, O. Shimmi, H. Nakato, Dally regulates Dpp morphogen gradient formation by stabilizing Dpp on the cell surface. *Dev. Biol.* **313**, 408–419 (2008).
23. A. Sarkar, N. Parikh, S. A. Hearn, M. T. Fuller, S. I. Tazuke, C. Schulz, Antagonistic roles of Rac and Rho in organizing the germ cell microenvironment. *Curr. Biol.* **17**, 1253–1258 (2007).
24. D. Yan, X. Lin, Shaping morphogen gradients by proteoglycans. *Cold Spring Harb. Perspect. Biol.* **1**, a002493 (2009).
25. M. I. Capurro, P. Xu, W. Shi, F. Li, A. Jia, J. Filmus, Glypican-3 inhibits Hedgehog signaling during development by competing with patched for Hedgehog binding. *Dev. Cell* **14**, 700–711 (2008).
26. E. H. Williams, W. N. Pappano, A. M. Saunders, M. S. Kim, D. J. Leahy, P. A. Beachy, Dally-like core protein and its mammalian homologues mediate stimulatory and inhibitory effects on Hedgehog signal response. *Proc. Natl. Acad. Sci. U.S.A.* **107**, 5869–5874 (2010).
27. M. Capurro, T. Martin, W. Shi, J. Filmus, Glypican-3 binds to Frizzled and plays a direct role in the stimulation of canonical Wnt signaling. *J. Cell Sci.* **127**, 1565–1575 (2014).
28. E. R. Olson, R. Pancratov, S. S. Chatterjee, B. Changkakoty, Z. Pervaiz, R. DasGupta, Yan, an ETS-domain transcription factor, negatively modulates the Wingless pathway in the *Drosophila* eye. *EMBO Rep.* **12**, 1047–1054 (2011).
29. P. Sahai-Hernandez, T. G. Nystul, A dynamic population of stromal cells contributes to the follicle stem cell niche in the *Drosophila* ovary. *Development* **140**, 4490–4498 (2013).

30. W. Dai, A. Peterson, T. Kenney, H. Burrous, D. J. Montell, Quantitative microscopy of the *Drosophila* ovary shows multiple niche signals specify progenitor cell fate. *Nat. Commun.* **8**, 1244 (2017).
31. V. Trivedi, H. M. T. Choi, S. E. Fraser, N. A. Pierce, Multidimensional quantitative analysis of mRNA expression within intact vertebrate embryos. *Development* **145**, dev15869 (2018).
32. C. Y. Tseng, Y. H. Su, S. M. Yang, K. Y. Lin, C. M. Lai, E. Rastegari, O. Amartuvshin, Y. Cho, Y. Cai, H. J. Hsu, Smad-independent BMP signaling in somatic cells limits the size of the germline stem cell pool. *Stem Cell Rep.* **11**, 811–827 (2018).
33. D. Yan, Y. Wu, Y. Feng, S. C. Lin, X. Lin, The core protein of glypican Dally-like determines its biphasic activity in wingless morphogen signaling. *Dev. Cell* **17**, 470–481 (2009).
34. D. Yan, Y. Wu, Y. Yang, T. Y. Belenkaya, X. Tang, X. Lin, The cell-surface proteins Dally-like and Ihog differentially regulate Hedgehog signaling strength and range during development. *Development* **137**, 2033–2044 (2010).
35. X. Song, M. D. Wong, E. Kawase, R. Xi, B. C. Ding, J. J. McCarthy, T. Xie, Bmp signals from niche cells directly repress transcription of a differentiation-promoting gene, bag of marbles, in germline stem cells in the *Drosophila* ovary. *Development* **131**, 1353–1364 (2004).
36. Y. Wu, T. Y. Belenkaya, X. Lin, Dual roles of *Drosophila* glypican Dally-like in Wingless/Wnt signaling and distribution. *Methods Enzymol.* **480**, 33–50 (2010).
37. D. Yan, X. Lin, Opposing roles for glypicans in Hedgehog signalling. *Nat. Cell Biol.* **10**, 761–763 (2008).
38. B. E. Housden, K. Millen, S. J. Bray, *Drosophila* reporter vectors compatible with ΦC31 integrase transgenesis techniques and their use to generate new notch reporter fly lines. *G3* **2**, 79–82 (2012).
39. M. Dominguez, M. Brunner, E. Hafen, K. Basler, Sending and receiving the hedgehog signal: Control by the *Drosophila* Gli protein Cubitus interruptus. *Science* **272**, 1621–1625 (1996).
40. C. Alexandre, A. Jacinto, P. W. Ingham, Transcriptional activation of hedgehog target genes in *Drosophila* is mediated directly by the cubitus interruptus protein, a member of the GLI family of zinc finger DNA-binding proteins. *Genes Dev.* **10**, 2003–2013 (1996).
41. E. Brunner, O. Peter, L. Schweizer, K. Basler, Pangolin encodes a Lef-1 homologue that acts downstream of Armadillo to transduce the Wingless signal in *Drosophila*. *Nature* **385**, 829–833 (1997).
42. E. Clough, T. Tedeschi, T. Hazelrigg, Epigenetic regulation of oogenesis and germ stem cell maintenance by the *Drosophila* histone methyltransferase Eggless/dSetDB1. *Dev. Biol.* **388**, 181–191 (2014).
43. U. Häcker, E. Kaufmann, C. Hartmann, G. Jürgens, W. Knöchel, H. Jäckle, The *Drosophila* fork head domain protein crocodile is required for the establishment of head structures. *EMBO J.* **14**, 5306–5317 (1995).
44. J. Jiang, G. Struhl, Protein kinase A and hedgehog signaling in *Drosophila* limb development. *Cell* **80**, 563–572 (1995).
45. R. T. Cox, L. M. Pai, J. R. Miller, S. Orsulic, J. Stein, C. A. McCormick, Y. Audeh, W. Wang, R. T. Moon, M. Peifer, Membrane-tethered *Drosophila* Armadillo cannot transduce Wingless signal on its own. *Development* **126**, 1327–1335 (1999).
46. K. K. Bluske, T. Y. Vue, Y. Kawakami, M. M. Taketo, K. Yoshikawa, J. E. Johnson, Y. Nakagawa, β-Catenin signaling specifies progenitor cell identity in parallel with Shh signaling in the developing mammalian thalamus. *Development* **139**, 2692–2702 (2012).
47. J. Rodriguez-Blanco, L. Pednekar, C. Penas, B. Li, V. Martin, J. Long, E. Lee, W. A. Weiss, C. Rodriguez, N. Mehrdad, D. M. Nguyen, N. G. Ayad, P. Rai, A. J. Capobianco, D. J. Robbins, Inhibition of WNT signaling attenuates self-renewal of SHH-subgroup medulloblastoma. *Oncogene* **36**, 6306–6314 (2017).
48. M. Ding, X. Wang, Antagonism between Hedgehog and Wnt signaling pathways regulates tumorigenicity. *Oncol. Lett.* **14**, 6327–6333 (2017).
49. K. Reynolds, P. Kumari, L. S. Rincon, R. Gu, Y. Ji, S. Kumar, C. J. Zhou, Wnt signaling in orofacial clefts: Crosstalk, pathogenesis and models. *Dis. Model. Mech.* **12**, dmm037051 (2019).
50. J. Jiang, G. Struhl, Complementary and mutually exclusive activities of decapentaplegic and wingless organize axial patterning during *Drosophila* leg development. *Cell* **86**, 401–409 (1996).
51. S. Takashima, R. Murakami, Regulation of pattern formation in the *Drosophila* hindgut by wg, hh, dpp, and en. *Mech. Dev.* **101**, 79–90 (2001).
52. H. Theisen, A. Syed, B. T. Nguyen, T. Lukacsovich, J. Purcell, G. P. Srivastava, D. Iron, K. Gaudenz, Q. Nie, F. Y. Wan, M. L. Waterman, J. L. Marsh, Wingless directly represses DPP morphogen expression via an armadillo/TCF/Brinker complex. *PLOS ONE* **2**, e142 (2007).
53. T. A. Blauwkamp, M. V. Chang, K. M. Cadigan, Novel TCF-binding sites specify transcriptional repression by Wnt signalling. *EMBO J.* **27**, 1436–1446 (2008).
54. H. Tanimoto, S. Itoh, P. ten Dijke, T. Tabata, Hedgehog creates a gradient of DPP activity in *Drosophila* wing imaginal discs. *Mol. Cell* **5**, 59–71 (2000).
55. F. Li, W. Shi, M. Capurro, J. Filmus, Glypican-5 stimulates rhabdomyosarcoma cell proliferation by activating Hedgehog signaling. *J. Cell Biol.* **192**, 691–704 (2011).
56. I. Strate, F. Tessadori, J. Bakkers, Glypican4 promotes cardiac specification and differentiation by attenuating canonical Wnt and Bmp signaling. *Development* **142**, 1767–1776 (2015).
57. Y. Han, Q. Shi, J. Jiang, Multisite interaction with Sufu regulates Ci/Gli activity through distinct mechanisms in Hh signal transduction. *Proc. Natl. Acad. Sci. U.S.A.* **112**, 6383–6388 (2015).
58. X. Ma, X. Zhu, Y. Han, B. Story, T. Do, X. Song, S. Wang, Y. Zhang, M. Blanchette, M. Gogol, K. Hall, A. Peak, P. Anoja, T. Xie, Aubergine controls germline stem cell self-renewal and progeny differentiation via distinct mechanisms. *Dev. Cell* **41**, 157–169.e5 (2017).
59. Y. Mao, R. Tu, Y. Huang, D. Mao, Z. Yang, P. K. Lau, J. Wang, J. Ni, Y. Guo, T. Xie, The exocyst functions in niche cells to promote germline stem cell differentiation by directly controlling EGFR membrane trafficking. *Development* **146**, dev174615 (2019).
60. S. G. Zimmerman, N. C. Peters, A. E. Altaras, C. A. Berg, Optimized RNA ISH, RNA FISH and protein-RNA double labeling (IF/FISH) in *Drosophila* ovaries. *Nat. Protoc.* **8**, 2158–2179 (2013).


**Acknowledgments:** We thank J. Jiang (UT Southwestern), D. Montell (UCSB Santa Barbara), TRiP (GM084947), Developmental Studies Hybridoma Bank and Bloomington *Drosophila* Stock Center for reagents, the Xie laboratory members for discussions, and K. Ishihara, R. Krumlauf, and A. Sánchez Alvarado for critical comments. **Funding:** This work was supported by Stowers Institute for Medical Research and a grant from the NIH (R01HD097664). **Author contributions:** R.T., B.D., and X.S. performed the experiments. R.T. and T.X. designed the experiments, analyzed the data, interpreted the data, and wrote the manuscript. **Competing interests:** The authors declare that they have no competing interest. **Data and materials availability:** All data needed to evaluate the conclusions in the paper are present in the paper and/or the Supplementary Materials. Additional data related to this paper may be requested from the authors. Original data underlying this study can be accessed from the Stowers Original Data Repository at http://www.stowers.org/research/publications/libpb-1512.

Submitted 7 August 2019
Accepted 28 February 2020
Published 13 May 2020
10.1126/sciadv.aaz0480

**Citation:** R. Tu, B. Duan, X. Song, T. Xie, Dlp-mediated Hh and Wnt signaling interdependence is critical in the niche for germline stem cell progeny differentiation. *Sci. Adv.* **6**, eaaz0480 (2020).